Index Modulated OFDM with ICI Self-Cancellation

Yuke Li[1,2], Miaowen Wen[3], Xiang Cheng[2,4], and Liu-Qing Yang[1,2,5]
[1]State Key Laboratory of Management and Control for Complex Systems,
Institute of Automation, Chinese Academy of Sciences, Beijing, 100190, China
[2]Qingdao Academy of Intelligent Industries, Qingdao, 266109, China.
[3]School of Electronic and Information Engineering,
South China University of Technology, Guangzhou, 510640, China
[4]School of Electronics Engineering and Computer Science, Peking University, Beijing, 100871, China
[5]Department of Electrical and Computer Engineering, Colorado State University, Fort Collins, CO 80523, USA
Email: liyuke14@mails.ucas.ac.cn, eemwwen@scut.edu.cn, xiangcheng@pku.edu.cn, liuqing.yang@ieee.org.

***Abstract*— Orthogonal frequency division multiplexing (OFDM) is prone to frequency offset which gives rise to intercarrier interference (ICI). Recently, a novel OFDM transmission scheme called OFDM with index modulation (IM-OFDM) is proposed, which outperforms conventional OFDM in the absence of frequency offset. As in IM-OFDM, partial subcarriers are set to be idle by spatial modulation, the potential of IM-OFDM in ICI reduction is expected. In this paper, we find that this potential vanishes in some real scenarios with ICI, which leads to IM-OFDM exhibiting even worse performance than conventional OFDM. To improve this situation, a novel ICI cancellation scheme is designed, which integrates the ICI self-cancellation technique into the IM-OFDM framework. Via careful designs, the proposed scheme not only provides a solution to ICI problems of IM-OFDM, but also achieves an attractive tradeoff between the spectral efficiency and ICI cancellation performance of the system. Simulations validate that in the presence of carrier frequency offset (CFO), the proposed scheme significantly outperforms existing IM-OFDM and more importantly shows better performance than the conventional OFDM with ICI self-cancellation.**

I. Introduction

OFDM has been widely adopted in modern wireless communication systems for extensive advantages it promises, e.g., capable of combatting the inter-symbol interference caused by the frequency-selective fading channel and easy to implement. However, by its nature that all subcarriers are strictly orthogonal, OFDM is prone to frequency offset caused by Doppler shift and/or transceiver imperfection. The frequency offset is very harmful to OFDM as it gives rise to ICI, which seriously degrades the system performance. To overcome this adverse effect, many ICI countermeasures have been proposed so far, such as time-domain windowing [1], frequency offset correction [2]–[4], and ICI self-cancellation [5], [6]. Among them, ICI self-cancellation has been widely accepted due to its simplicity and effectiveness in ICI reduction [7], [8].

Recently, significant effort has been devoted to extending the idea of spatial modulation, which belongs to the multi-input-multi-output (MIMO) family and is widely accepted as a candidate for 5G transmission techniques [9]–[11], to OFDM. The first attempt was made in [12] and [13], where a scheme called subcarrier-index modulation- (SIM-)OFDM is proposed. Later, SIM-OFDM was generalized as IM-OFDM in [14]. To ease the implementation of IM-OFDM, the OFDM block is split into subblocks such that subcarrier activation and symbol modulation can be performed within each subblock independently. In each subblock, partial subcarriers are selected to be active/inactive randomly according to incoming information bits and the active subcarriers carry M-ary phase shift keying/quadrature amplitude modulation (PSK/QAM) symbols as in conventional OFDM. Therefore, both the M-ary signal constellation and the indices of the subcarriers carry information, rendering IM-OFDM superior to conventional OFDM in terms of both BER and error-free achievable rate in the absence of ICI [15].

Due to the fact that partial subcarriers are idle, IM-OFDM has less number of active subcarriers than plain OFDM at any time, which provides IM-OFDM with the potential of ICI reduction. However, in the presence of frequency offset, ICI enhances the received signal power of each inactive subcarriers and reduces that of each active subcarriers, making subcarrier states very difficult to differentiate and further misleading the detection of the transmitted symbols on the active subcarriers. This will significantly deteriorate the system performance and make it even worse than conventional OFDM. Therefore, how to properly deal with ICI is a very important issue for the practical use of IM-OFDM and still an open research problem.

ICI self-cancellation technique provides a possible solution to the aforementioned problem. The main idea of ICI self-cancellation is to modulate one data symbol onto two adjacent subcarriers with predefined weighting coefficients so that the ICI signals generated within neighboring subcarriers can be self-cancelled each other. With ICI self-cancellation method, the ICI level experienced by the inactive subcarriers in IM-OFDM is expected to be reduced. In addition, the performance of ICI self-cancellation could be improved due to a smaller number of active subcarriers by the nature of IM-OFDM. In order to create this win-win situation, we propose a novel ICI self-cancellation scheme that successfully integrates ICI self-cancellation method into the IM-OFDM architecture. Being aware that the method proposed in [14] for subcarrier grouping is suboptimal in the sense of BER performance, we suggest

978-1-5090-1698-3/16/$31.00 ©2016 IEEE

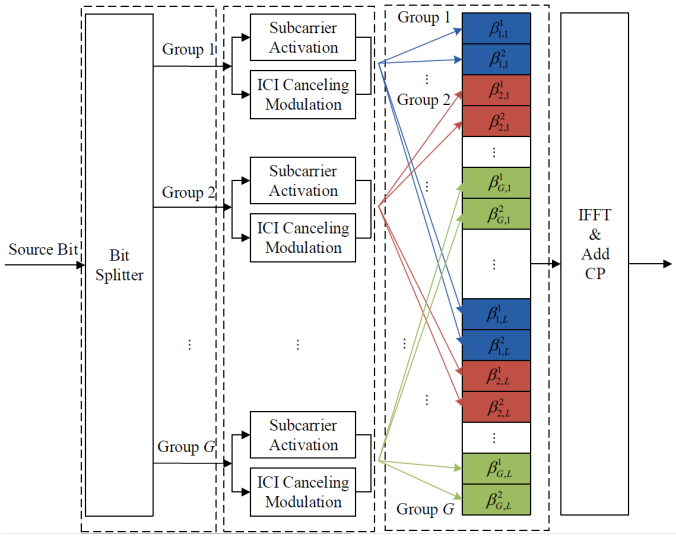

Fig. 1. Transmitter structure of the proposed scheme.

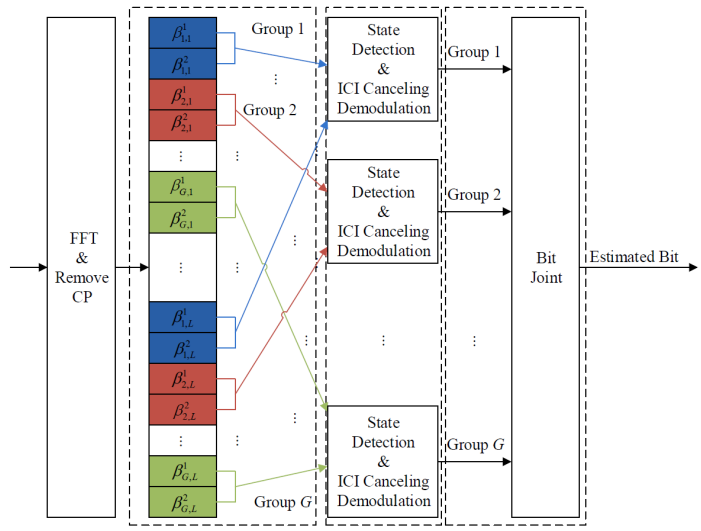

Fig. 2. Receiver structure of the proposed scheme.

grouping subcarriers in an interleaved manner for the proposed scheme to facilitate a higher achievable rate and significant performance improvement [16]. The developed IM-OFDM with ICI self-cancellation scheme can not only properly deal with the ICI problem in IM-OFDM systems, but also performs much better system performance than IM-OFDM and ICI self-cancellation. To better demonstrate the idea, we assume that the systems suffer from the CFO caused by the mismatch between the frequency of the received signal and that of the oscillator. It is shown through analysis that the ICI experienced by the proposed system can be suppressed to a very low level with the help of ICI self-cancellation and spatial modulation. Simulations over different CFO scenarios show that the proposed scheme significantly outperforms existing IM-OFDM and OFDM with ICI self-cancellation.

II. SYSTEM MODEL

Suppose that there are in total N OFDM subcarriers. The transmission is initialized by dividing the subcarriers into G subblocks, of which each contains L subcarrier pairs (SPs). It is worth noting that the subcarriers are defined pair-wise in the proposed scheme. Each SP contains two adjacent subcarriers, such that $N = 2GL$. Denote the index of the l-th SP within g-th subblock as $\beta_{g,l}$, where $g = 1, 2, \cdots, G$ and $l = 1, 2, \cdots, L$. In each SP, the index of the first subcarrier is denoted by $\beta^1_{g,l}$, and the other one $\beta^2_{g,l}$, such that $\beta_{g,l} = \{\beta^1_{g,l}, \beta^2_{g,l}\}$.

A. Transmitter structure

Fig.1 shows the transmitter structure of the proposed scheme. At the very beginning, the incoming source bits are fed into the bit splitter. Suppose that there are q bits in total, they are divided into G groups, of which each contains two parts: p_1 bits and p_2 bits. Therefore, $q = G(p_1 + p_2)$. Then, the first part p_1 will determine the state of all subcarriers and the second part p_2 will modulate the symbols transmitted on the active subcarriers within a subcarrier subblock. Details on how they work will be presented in the following by taking group g and subcarrier subblock g as a demonstrative example, where $g = 1, \cdots, G$.

The first part p_1 renders m out of L SPs active, and the remaining $L - m$ SPs inactive. It is worth noting that the subcarrier state is determined pair-wise in the proposed scheme, which means the two neighboring subcarriers within one SP share the same state. Note that given L and m, there are in total $\mathrm{C}(L, m)$ different combinations of active/inactive subcarrier indices, and only $2^{\lfloor \log_2 \mathrm{C}(L,m) \rfloor}$ of them are taken into account, yielding $p_1 = \lfloor \log_2 \mathrm{C}(L, m) \rfloor$.

Example: Take $L = 4$ and $m = 2$ for example. All $\mathrm{C}(4, 2) = 6$ combinations for subcarrier subblock g are listed as follows:

TABLE I

A LOOK-UP TABLE FOR $L = 4, m = 2$

1	$I_g = \{\beta_{g,1}, \beta_{g,2}\}$	$\bar{I}_g = \{\beta_{g,3}, \beta_{g,4}\}$
2	$I_g = \{\beta_{g,1}, \beta_{g,3}\}$	$\bar{I}_g = \{\beta_{g,2}, \beta_{g,4}\}$
3	$I_g = \{\beta_{g,1}, \beta_{g,4}\}$	$\bar{I}_g = \{\beta_{g,2}, \beta_{g,3}\}$
4	$I_g = \{\beta_{g,2}, \beta_{g,3}\}$	$\bar{I}_g = \{\beta_{g,1}, \beta_{g,4}\}$
5	$I_g = \{\beta_{g,2}, \beta_{g,4}\}$	$\bar{I}_g = \{\beta_{g,1}, \beta_{g,3}\}$
6	$I_g = \{\beta_{g,3}, \beta_{g,4}\}$	$\bar{I}_g = \{\beta_{g,1}, \beta_{g,2}\}$

where $g = 1, \cdots, G$, I_g represents the indices of active SPs for subcarrier group g, and $\bar{I}_g$ represents the complement of I_g, which consists of indices of inactive SPs. Only $\lfloor \log_2 \mathrm{C}(4, 2) \rfloor = 4$ of 6 combinations are taken into account, yielding $p_1 = 2$ bits. Assume that the first coming p_1 bits is "01". Convert p_1 bits into a decimal and plus 1, then the 3rd index combination in the table is selected. However, the table will become very huge as L grows, rendering this look-up table method impractical. Under this circumstance, the combinatorial method is recommended. Details about combinatorial method can be found in [14].

The second part p_2 generates $(L-m)$ M-ary modulated symbols, which implies that $p_2 = m\log_2 M$, where M is the cardinality of the constellation. Due to the fact that the difference between the ICI coefficients of adjacent subcarrier is very small, the ICI signal is expected to be self-cancelled within adjacent subcarriers. Therefore, a data pair, such as $(a,-a)$ is modulated onto $\beta_{g,l}$-th SP, where $\beta_{g,l} = \{\beta^1_{g,l}, \beta^2_{g,l}\}$ and $\beta_{g,l} \in I_g$. Denote the $\beta_{g,l}$-th transmitted signal pair as $S_{\beta_{g,l}}$, thus $S_{\beta_{g,l}} = \{S_{\beta^1_{g,l}}, S_{\beta^2_{g,l}}\} = \{S_{\beta^1_{g,l}}, -S_{\beta^1_{g,l}}\}$. By this design following the ICI self-cancellation technique [5], the ICI generated within each SP is expected to be cancelled out significantly. Taking subcarrier activation and M-ary modulation into account, each group conveys $p_1+p_2 = \lfloor \log_2 \mathrm{C}(L,m) \rfloor + m\log_2 M$ bits. Consequently, the spectral efficiency achieved by the proposed scheme is given by (bps/Hz)

$$f = \frac{\lfloor \log_2 \mathrm{C}(L,m) \rfloor}{2L} + \frac{m\log_2 M}{2L}. \tag{1}$$

We consider interleaved grouping for its optimality among all possible subcarrier grouping methods. Equal-spaced SPs in frequency are collected to form a group:

$$\{S_{\beta_{1,1}}, S_{\beta_{2,1}}, \cdots, S_{\beta_{G,1}}, S_{\beta_{1,2}}, S_{\beta_{2,2}}, \cdots, S_{\beta_{G,2}}, \cdots, S_{\beta_{1,L}}, S_{\beta_{2,L}}, \cdots, S_{\beta_{G,L}}\}$$

Denote the transmitted signals on frequency domain as $X(k)$, where $k = 1,2,\ldots,N$. The transmitted signals at all subcarriers are given by

$$\mathbf{X} = [X(1),\ldots,X(N)]^T \tag{2}$$

where $g = 1,\cdots,G$, $l = 1,\cdots,L$, and $(\cdot)^T$ stands for the transpose operation. Before transmission, the inverse fast Fourier transform (FFT) is applied to (2). Then, a cyclic prefix (CP) is added to the beginning of the time-domain OFDM symbol.

B. Receiver structure

Fig. 2 shows the receiver structure of the proposed scheme. At the receiver, the CP of the received signal is first removed and the application of the FFT is followed. The received signal at the k-th subcarrier can be expressed as:

$$Y(k) = H(k)X(k)C(0) + \sum_{i=1, i\neq k}^{N} H(i)X(i)C(i-k) + W(k), \tag{3}$$

where $H(k)$ represents the channel frequency response (CFR) at the k-th subcarrier and $W(k)$ is the noise in the frequency domain, where $k = 1,2,\cdots,N$. The second term at the right-hand side of (3) represents the ICI, where $C(i-k)$ is the ICI coefficient, given by

$$C(i-k) = \frac{\sin(\pi(i+\varepsilon-k))}{N\sin\left(\frac{\pi}{N}(i+\varepsilon-k)\right)} \cdot \exp\left(\frac{j\pi(N-1)(i+\varepsilon-k)}{N}\right), \tag{4}$$

where ε is the normalized CFO to the subcarrier spacing.

Denote the $\beta_{g,l}$-th received signal pair as $R_{\beta_{g,l}} = \{R_{\beta^1_{g,l}}, R_{\beta^2_{g,l}}\}$. The received signals at all subcarriers are given by

$$\mathbf{Y} = [Y(1),\ldots,Y(N)]^T \tag{5}$$

Next, all received signals are grouped in an interleaved manner similar to the operations performed at the transmitter. That is, all received signals are extracted as:

$$\{R_{\beta_{1,1}}, R_{\beta_{1,2}}, \cdots, R_{\beta_{1,L}}, \cdots, R_{\beta_{G,1}}, R_{\beta_{G,2}}, \cdots, R_{\beta_{G,L}}\}$$

Then, the ICI canceling demodulation is executed within each SP, yielding

$$R'_{\beta_{g,l}} = \frac{1}{2}\left(R_{\beta^1_{g,l}} - R_{\beta^2_{g,l}}\right). \tag{6}$$

In this manner, the residual ICI in the received signals can be further reduced.

Next, the joint detection of the subcarrier states and the modulated symbols is carried out based on the maximum-likelihood (ML) detector and log-likelihood ratio (LLR) detector. For brevity, we take subcarrier group g as a demonstrative example in the following, where $g \in \{1,2,\cdots,G\}$. It can be presented as follows:

1) ML detector: The ML detector considers all possible subblock to make a joint decision on the active indices and the constellation symbols, denoted as $\hat{I}_g$ and $\hat{S}_g$ respectively. For group g, there are $\mathrm{C}(L,m)$ index combinations of active SPs, denoted by Φ^g_b, where $b = 1,2,\cdots,\mathrm{C}(L,m)$. Let $\bar{\Phi}^g_b$ denote the complement of Φ^b_g. The ML detector can be derived as:

$$\left\langle \hat{I}_g, \hat{S}_g \right\rangle = \arg\min_{b\in\Theta} \sum_{\beta_{g,l}\in\Phi^g_b} \left| R'_{\beta_{g,l}} - H'_{\beta_{g,l}} \hat{S}_{\beta_{g,l}} \right|^2 + \sum_{\beta_{g,l}\in\bar{\Phi}^g_b} \left| R'_{\beta_{g,l}} \right|^2, \tag{7}$$

where $\Theta = \{1,2,\cdots,\mathrm{C}(L,m)\}$ and $H'_{\beta_{g,l}}$ is the CFR at the $\beta_{g,l}$-th SP, defined as $H'_{\beta_{g,l}} = \frac{1}{2}\left(\hat{H}_{\beta^1_{g,l}} + \hat{H}_{\beta^2_{g,l}}\right)$, with $\hat{H}_{\beta^1_{g,l}}$ and $\hat{H}_{\beta^2_{g,l}}$ denoting the channel estimates on the corresponding subcarriers. In (7), $\hat{S}_{\beta_{g,l}}$ is the estimated transmitted signal carried on the $\beta_{g,l}$-th SP, which can be obtained by searching for the closest constellation point to $R'_{\beta_{g,l}}$, which means,

$$\hat{S}_{\beta_{g,l}} = \arg\min_{x_\alpha\in\chi} \left| R'_{\beta_{g,l}} - H'_{\beta_{g,l}} x_\alpha \right|^2, \tag{8}$$

where $\alpha = 1,\cdots,M$ and χ denotes the complex signal constellation of size M.

It is clear that the total computational complexity of the ML detector in (7), in terms of complex multiplications, is $\mathcal{O}(\mathrm{C}(L,m)M^m)$ per subblock since $\hat{I}_g$ and $\hat{S}_g$ have $\mathrm{C}(L,m)$ and M^m realizations, respectively. Therefore, the ML detector becomes impractical for larger values of L and m due to its exponentially growing decoding complexity.

2) LLR detector: To reduce the computational complexity futher, LLR detector is redesigned for the proposed scheme. The idea of LLR detector is to perform the aforementioned detections in a serial manner. Specifically, the first step is to detect the state of the $\beta_{g,l}$-th SP by examining the LLR value

$$\lambda_{\beta_{g,l}} = \ln(m) - \ln(L-m) + \frac{2|R'_{\beta_{g,l}}|^2}{N_0} + \ln\left(\sum_{\alpha=1}^{M} \exp\left(-\frac{2}{N_0}|R'_{\beta_{g,l}} - H'_{\beta_{g,l}} x_\alpha|^2\right)\right) \tag{9}$$

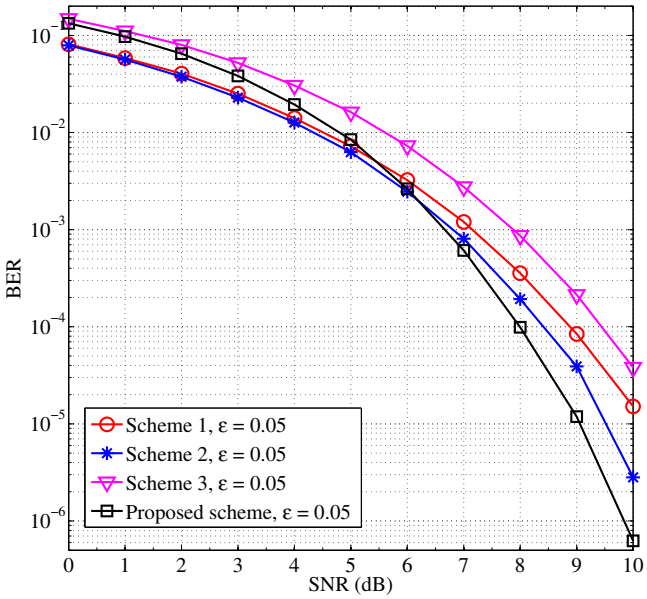

Fig. 3. Comparison of BERs achieved by the four schemes under $\varepsilon = 0.05$ over AWGN channel.

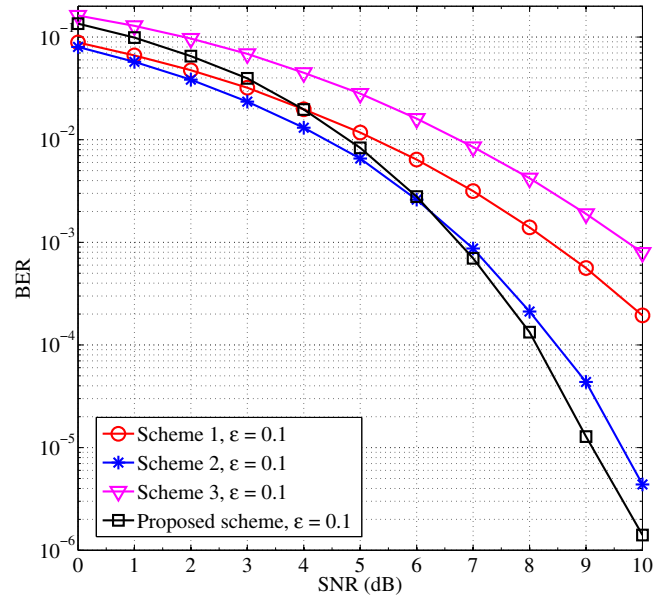

Fig. 4. Comparison of BERs achieved by the four schemes under $\varepsilon = 0.1$ over AWGN channel.

Note that the ICI self-cancel demodulation in (6) amplifies the noise power so the noise power in (9) should multiply by a factor of 2. Then, the m SPs within the g-th subblock having maximum LLR values are determined to be active. The second step is to demodulate the received signals associated with the subcarriers determined to be active in the first step. It can be readily shown that the computational complexity of the LLR detector is $\mathcal{O}(LM)$ per subblock, which is the same as that of the conventional OFDM detector. It has been proved that the LLR detector exhibits the same BER performance as ML detector [14].

III. Simulation Results and Analysis

This section presents BER simulation results for the proposed scheme. In the simulations, the total number of subcarriers is set to be $N = 64$ and the LLR detector is adopted for its speediness. For the proposed scheme, the system parameters are chosen as: $G = 8$, $L = 4$, $m = 3$, and QPSK modulation. The proposed scheme will be compared to these three other schemes as follows:

- Scheme 1: OFDM with BPSK modulation;
- Scheme 2: OFDM with ICI self-cancellation and QPSK modulation;
- Scheme 3: IM-OFDM with four subcarriers as a group, two subcarriers activated, and BPSK modulation

It can be readily figured out that the proposed scheme shares the same spectral efficiency, i.e., 1 bps/Hz, as the above three schemes. Therefore, the comparison is fair in this sense. In the simulations, the channel estimation is performed by the preamble, which is located prior to each OFDM data symbol and comprises an entire OFDM symbol known by both the transmitter and the receiver. We measured BERs achieved by the aforementioned four schemes versus different values of SNR, which is defined as $\gamma = P/NN_0$, where N_0 is the variance of the additive white Gaussian noise (AWGN) experienced by per subcarrier, and obtained the following results.

Figs. 3 and 4 show the comparison results under $\varepsilon = 0.05$ and 0.1 over AWGN channels, respectively. As can be seen, the IM-OFDM performs worse than other schemes. This can be understood since with the existence of CFO, the power of the received signal at each inactive subcarrier is enhanced, rendering subcarrier states difficult to distinguish, which seriously deteriorates the system performance and makes it even worse than Scheme 1. Therefore, it is not surprising to observe a similar phenomenon in Figs. 4 and 5. On the other hand, we see from Fig. 3 that Scheme 2 performs better than Scheme 1, which validates the effectiveness of the ICI self-cancellation technique in ICI reduction. However, it is revealed that when BER falls below 10^{-3}, the effect of ICI self-cancellation within the proposed scheme appears and the proposed scheme shows better performance than other schemes.

Fig. 4 shows the comparison result under $\varepsilon = 0.1$ over AWGN channels. We see that as the ICI becomes dominant, Schemes 1 and 3 cannot work normally due to the serious ICI signal. With the adoption of the ICI self-cancellation technique, however, Scheme 2 and the proposed scheme perform very well as we expect.

Fig. 5 shows the comparison results under $\varepsilon = 0.05$ and $\varepsilon = 0.2$ over the multipath fading channels, where symbol spaced, tap-delay-line channel model of eight paths and exponential power delay profile is used and each tap is an independent complex Gaussian variable. From Fig. 5, it is shown that IM-OFDM performs even worse than conventional OFDM, and thus loses it competitiveness in the presence of CFO. With the adoption ICI self-cancellation method, Scheme 2 and

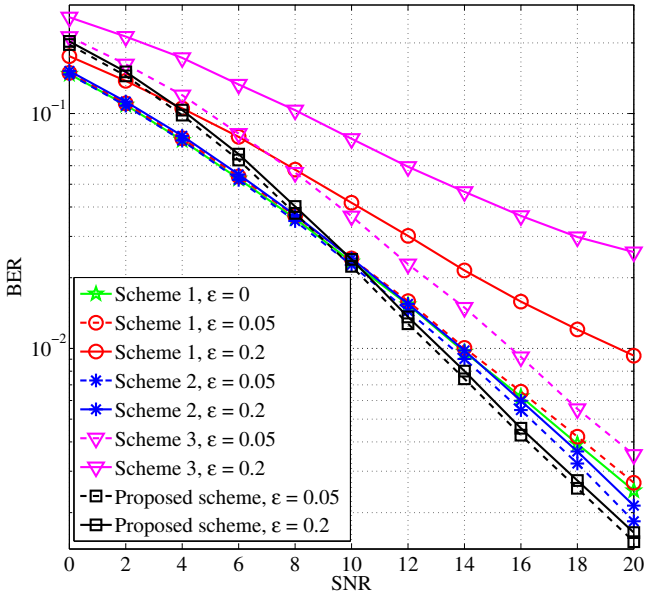

Fig. 5. Comparison of BERs achieved by the four schemes under $\varepsilon = 0.05$ and $\varepsilon = 0.2$ over multipath fading channels.

the proposed scheme outperform Scheme 1 and Scheme 3. When BER falls below 10^{-2}, the proposed scheme performs better than Scheme 2. It can be understood since that a smaller number of active subcarriers which actually incur ICI is achieved in the proposed scheme. More surprisingly, it is shown that the proposed scheme under $\varepsilon = 0.2$ performs even better than Scheme 2 under $\varepsilon = 0.05$.

Remark 2: It is clear from Figs. 3-5 that the proposed scheme outperforms conventional OFDM and IM-OFDM. This can be understood since with ICI self-cancellation, the ICI generated from adjacent subcarriers is suppressed. In addition, the proposed scheme performs even better than OFDM with ICI self-cancellation in the moderate-to-high SNR region. This is as expected because in the proposed scheme, almost $N(L-m)/L$ subcarriers transmit zero energy and the number of active subcarriers which actually incur ICI is reduced to $(m/L)N$.

Remark 3: The reason why the proposed scheme performs worse than OFDM with ICI self-cancellation in the low-to-moderate SNR region can be explained by the suboptimal detection in (9). This sub-optimality is due to the fact that (9) is based on the LLR criterion, which is valid only in the absence of CFO. Therefore, performance penalty arises in the presence of CFO. On the other hand, when the SNR is low, the noise largely contributes to the power of received signals. Consequently, the power of the received signal at each inactive subcarrier becomes comparable to that at each active subcarrier, which also misleads the detection of subcarrier states.

IV. Conclusions

We have proposed a novel ICI cancellation scheme which integrates the ICI self-cancellation technique into IM-OFDM systems for combatting ICI arising from CFO. The transceiver structure of the proposed scheme has been designed. Through BER simulations, it has been verified that the proposed scheme not only solves the ICI problem of IM-OFDM in the presence of CFO but also achieves better BER performance than OFDM with ICI self-cancellation.

V. Acknowledgement

This work was supported in part by the National Natural Science Foundation of China under Grants 61571020 and 61501461; by the National Science Foundation under Grant CNS-1343189; by the National 973 Project under Grant 2013CB336700; and by the Early Career Development Award of SKLMCCS (Y3S9021F34).

References

[1] R. Li and G. Stette, "Time-limited orthogonal multicarrier modulation schemes," *IEEE Trans. Commun.*, vol. 43, no. 234, pp. 1269–1272, Jul. 1995.

[2] J. J. van de Beek, M. Sandell, and P. O. Borjesson, "ML estimation of time and frequency offset in OFDM systems,"*IEEE Trans. Signal Process.*, vol. 45, no. 7, pp. 1800–1805, Jul. 1997.

[3] U. Tureli, D. Kivanc, and H. Liu, "Experimental and analytical studies on a high-resolution OFDM carrier frequency offset estimator,"*IEEE Trans. on Veh. Tech.*, vol. 50, no. 2, pp. 629–643, Mar. 2001.

[4] M. Luise, M. Marselli, and R. Reggiannini, "Low-complexity blind carrier frequency recovery for OFDM signals over frequency-selective radio channels," *IEEE Trans. Commun.*, vol. 50, no. 7, pp. 1182–1188, Jul. 2002.

[5] Y. Zhao, S-G. Haggman, "Intercarrier interference self-cancellation scheme for OFDM mobile communication systems," *IEEE Trans. Commun.*, vol. 49, no. 7, pp. 1185–1191, Jul. 2001.

[6] M. Wen, X. Cheng, X. Wei, B. Ai, and B. Jiao, "A novel effective ICI self-cancellation method," in *Proc. IEEE Globecom'11*, Houston, USA, Dec. 2011.

[7] X. Cheng, Q. Yao, M. Wen, C. X. Wang, L. Song, and B. Jiao, "Wideband channel modeling and ICI cancellation for vehicle-to-vehicle communication systems," *IEEE J. Sel. Areas in Commun.*, vol. 31, no. 9, pp. 434-448, Sept. 2013.

[8] X. Cheng, M. Wen, X. Cheng, D. Duan, and L. Yang, "Effective mirror-mapping-based intercarrier interference cancellation for OFDM underwater acoustic communications," *Ad Hoc Networks (Elsevier)*, vol. 34, pp. 5-16, Nov. 2015.

[9] R. Mesleh, H. Haas, S. Sinanović, C. W. Ahn, and S. Yun, "Spatial modulation," *IEEE Trans. on Veh. Tech.*, vol. 57, no. 4, pp. 2228–2241, Jul. 2008.

[10] M. Di Renzo, H. Haas, A. Ghrayeb, S. Sugiura, and L. Hanzo, "Spatial modulation for generalized MIMO: Challenges, opportunities and implementation," *Proc. of the IEEE*, vol. 102, no. 1, pp. 56-103, Jan. 2014.

[11] C. X. Wang, F. Haider, X. Gao, X. You, Y. Yang, D. Yuan, H. Aggoune, H. Haas, S. Fletcher, and E. Hepsaydir, "Cellular architecture and key technologies for 5G wireless communication networks," *IEEE Commun. Mag.*, vol. 52, no. 2, pp. 122-130, Feb. 2014.

[12] R. A. Alhiga and H. Haas, "Subcarrier-index modulation OFDM," in *Proc. IEEE PIMRC*, Tokyo, Japan, 2009, pp. 177-181.

[13] D. Tsonev, S. Sinanovic, and H. Haas, "Enhanced subcarrier index modulation (SIM) OFDM," in *Proc. IEEE GLOBECOM Workshops*, Houston, USA, 2011, pp. 728-732.

[14] E. Basar, U. Aygolu, E. Panayirci, and H. V. Poor, "Orthogonal frequency division multiplexing with index modulation," *IEEE Trans. Signal Process.*, vol. 61, no. 22, pp. 5536-5549, Nov. 2013.

[15] M. Wen, X. Cheng, and L. Yang, "Optimizing the Energy Efficiency of OFDM with Index Modulation," in *Proc. IEEE ICCS 2014*, Macau, China, Nov. 2014, pp. 31-35.

[16] X. Cheng, M. Wen, L. Yang, and Y. Li, "Index Modulated OFDM with Interleaved Grouping for V2X Communications," in *Proc. IEEE ITSC 2014*, Qingdao, China, Oct. 2014, pp. 1097-1104.